Earth-science Reviews
February 2021, Volume 213 Pages 103464 (12p.)
https://doi.org/10.1016/j.earscirev.2020.103464
https://archimer.ifremer.fr/doc/00744/85648/

Insights into soft-part preservation from the Early Ordovician Fezouata Biota

Saleh Farid [1, 2, 3, *], Vaucher Romain [4], Antcliffe Jonathan B. [5], Daley Allison C. [5], El Hariri Khadija [6], Kouraiss Khaoula [6], Lefebvre Bertrand [3], Martin Emmanuel L. O. [3], Perrillat Jean-Philippe [3], Sansjofre Pierre [7], Vidal Muriel [8], Pittet Bernard [3]

[1] Yunnan Key Laboratory for Palaeobiology, Institute of Palaeontology, Yunnan University, Kunming, China
[2] MEC International Joint Laboratory for Palaeobiology and Palaeoenvironment, Institute of Palaeontology, Yunnan University, Kunming, China
[3] Université de Lyon, Université Claude Bernard Lyon 1, École Normale Supérieure de Lyon, CNRS, UMR5276, LGL-TPE, Villeurbanne, France
[4] Applied Research in Ichnology and Sedimentology (ARISE) Group, Department of Earth Sciences, Simon Fraser University, Burnaby, British Columbia V5A 1S6, Canada
[5] Institute of Earth Sciences, University of Lausanne, Géopolis, CH-1015 Lausanne, Switzerland
[6] Laboratoire de Géosciences et Environnement, Faculté des Sciences et Techniques, Université Cadi-Ayyad, BP 549, 40000 Marrakesh, Morocco
[7] MNHN, Sorbonne Université, CNRS UMR 7590, IRD, Institut de Minéralogie, Physique des Matériaux et de Cosmochimie, Paris, France
[8] Univ. Brest, CNRS, IUEM Institut Universitaire Européen de la Mer, UMR 6538 Laboratoire Géosciences Océan, Place Nicolas Copernic, 29280 Plouzané, France

* Corresponding author : Farid Saleh, email address : farid.nassim.saleh@gmail.com

Abstract :

The Fezouata Biota in Morocco is the only Lower Ordovician Lagerstadtte yielding a biologically diverse assemblage in a fully marine environment, whilst also containing organisms typical of Cambrian Burgess Shale-type (BST) ecosystems. Fossils from the Fezouata Shale share the same mode of preservation as Cambrian BST biotas defined by carbonaceous compressions and accessory authigenic mineralization. Most organisms of the Fezouata Biota were already dead and decaying on the seafloor when they were buried in-situ by occasional storm-induced deposits in an environment just below the storm-weather wave base. Pre-burial decay in the Fezouata Shale was responsible for the non-preservation of completely cellular organisms such as jellyfish. These conditions contrast with the processes described for soft-tissue preservation in the Burgess Shale (Canada) and the Chengjiang Biota (China). In these two Cambrian Lagerstadtten, animals were transported alive or shortly after death by obrution events to an environment that was favorable for preservation. Despite preservational biases, the autochthonous assemblages of the Fezouata Shale offer a unique opportunity to decipher the structure of in situ communities and ecological dynamics in Early Palaeozoic seas, when compared to the allochthonous communities of most Cambrian BST biotas.

Keywords : Exceptional preservation, Cambrian, Fezouata Shale, Burgess Shale, Chengjiang Biota, Taphonomy

1. Introduction

Fossils are key elements in deciphering ancient life on Earth. Much of our knowledge on biodiversification and extinction events comes from mineralized parts such as bones and shells because these are relatively abundant and are commonly found around the globe (Fan et al., 2020). However, organisms having mineralized parts constituting at least part of their bodies are not the sole components in modern ecosystems. A large number of animals are completely soft, having either cuticularized body walls (i.e. formed of polysaccharides), such as annelids and priapulids, or even entirely cellular bodies, such as jellyfish (e.g. Liu et al., 2008; Zhang et al., 2008; Lamsdell et al., 2013; Duan et al., 2014; Lei et al., 2014; Gutiérrez-Marco and García-Bellido, 2015; Martin et al., 2016a; Lerosey-Aubril et al., 2017). Thus, studies based on mineralized parts in the fossil record provide incomplete samples of past animal life on Earth. For this reason, incorporating information from localities with exceptional fossil preservation yielding labile anatomies is crucial to reconstruct ancient ecosystems more accurately (Daley et al., 2018). Although generally rare over the geological time scale, exceptionally preserved biotas discovered in deposits called “Lagerstätten” are common in the Cambrian (Gaines, 2014). The most famous Cambrian site with exceptional preservation is the Burgess Shale (Miaolingian, Canada; Butterfield 1990, 1995; Conway Morris, 1992; Gaines, 2014). The discovery of soft animal taxa in this locality transformed palaeontological knowledge on the earliest eumetazoan-dominated communities during the Cambrian Explosion (e.g. Daley et al., 2009, 2018; Smith and Caron, 2010; Moysiuk et al., 2017; Moysiuk and Caron, 2019; Nanglu et al., 2020). In the last 40 years, over 50 Burgess Shale-type (BST) assemblages have been discovered, most of them from the early to middle Cambrian (Gaines, 2014). Fossils from the Chengjiang Biota (Cambrian Series 2, China) preserved tissues that decay fast in laboratory conditions, and shed light on the early evolution of numerous metazoan phyla (Hou et al., 2004). For instance, nervous tissues were discovered

in different arthropod groups ending long-standing debates on the systematic affinities of these taxa (Ma et al., 2012, 2015; Tanaka et al., 2013; Cong et al., 2014). The Chengjiang Biota yielded also the best fossilized cardiovascular system ever discovered (Ma et al., 2014). All these animals from Cambrian BST assemblages were preserved under similar environmental conditions and share the same mode of preservation (Gaines et al., 2008, 2012a). They were transported from their living environment, alive or shortly after their death by obrution events, to another setting, where they were buried and eventually preserved (Gaines, 2014). The rapid transport and burial of these animals provided a very limited time for oxic decay to occur, and increased the chances of tissues to escape oxygen in the water column of their original environment (Gaines, 2014). In the deeper facies where they were buried, anoxia was permissive at least at the sea bottom, and carbonate cement precipitated on top of burial event deposits blocking exchange between the water column and sediments and inhibiting oxidants from attaining decaying carcasses (Gaines et al., 2012a). It was also recently suggested that specific clay minerals may have helped BST preservation by slowing down bacterial decay (McMahon et al., 2016). Thus, carcasses were isolated in a fine-grained lithology allowing their preservation in minute details as carbonaceous compressions (Gaines et al., 2008). In some cases, authigenic mineralization (i.e. pyritization, phosphatization) may have occurred, but this remained accessory to the primary carbonaceous mode of preservation (Gaines et al., 2008). Then, for some sites (i.e. the Burgess Shale, and Sirius Passet), the compressed organic matter was kerogenized and matured under metamorphic conditions at temperatures between 300 and 400 degrees (Topper et al., 2018). Although the general conditions for exceptional fossil preservation are relatively well-known for Cambrian Lagerstätten, the mechanisms at play for soft-tissue preservation in younger BST deposits remain largely unexplored.

In the early 2000s, a new Lagerstätte was discovered in the Zagora area, Central Anti-Atlas of Morocco. The Fezouata Shale is, so far, the only unit to yield a highly diverse, fully marine exceptionally preserved Ordovician biota (Van Roy et al., 2010, 2015a; Lefebvre et al., 2016a; Martin et al., 2016a). With more than 185 taxa of marine invertebrates recovered from numerous sites in the Zagora area, this formation offers new insights into the diversification of metazoans, at a key interval between the Cambrian Explosion and the Ordovician Radiation (Van Roy et al., 2010, 2015a; Lefebvre et al., 2016a). Most of these taxa are shelly organisms typical of the Ordovician Radiation including asterozoans, bivalves, rhynchonelliformean brachiopods, cephalopods, crinoids, gastropods, graptolites, ostracods, and trilobites (Fig. 1). The Fezouata Biota also comprises a high number of soft-bodied to lightly sclerotized taxa (Fig. 1). Some of these exceptionally preserved organisms (e.g. cirriped crustaceans, eurypterid and xiphosuran chelicerates) represent the oldest occurrences of important marine invertebrate groups, previously only recorded from younger Lagerstätten (Van Roy et al., 2015a). The Fezouata Biota also includes abundant representatives of taxa typical of Cambrian age BST Lagerstätten (e.g. radiodonts, protomonaxonids, armored lobopodians, marrellomorphs, naraoiids) (Botting, 2007, 2016; Vinther et al., 2008, 2017; Van Roy et al., 2010, 2015b; Pérez-Peris et al., in press).

Two modes of exceptional preservation have been documented in the Fezouata Shale. The first one occurs in concretions (Gaines et al., 2012b). The second type of exceptional preservation is associated with shales in a generally shallower environment in comparison to the classical Burgess Shale (Martin et al., 2016a; Vaucher et al., 2016). Most Fezouata BST fossils collected in shales are preserved as molds or imprints on the sediments (Martin et al., 2016a), and it is unclear whether these organisms were originally preserved as carbonaceous compressions. In some cases, some non-biomineralized tissues in flattened fossils, such as

117 trilobite digestive tracts and echinoderm water-vascular systems, are preserved in 3D iron
118 oxides (Van Roy et al., 2010; Gutiérrez-Marco et al., 2017; Lefebvre et al., 2019).
119 Considering that numerous mechanisms may favor or alter the preservation of original
120 anatomies in fossils (Fig. 2), deciphering the taphonomic processes is essential for
121 palaeontological and ecological studies, especially for taxa without extant representatives.
122 Consequently, the aim of this study is to review soft tissue taphonomy in the Fezouata Shale
123 based on a multidisciplinary approach combining data across palaeontology, sedimentology,
124 geochemistry and mineralogy. This in-depth reconstruction starts at the life of an organism in
125 its environment and ends at its discovery in surface sediments passing through biostratinomy,
126 diagenesis, metamorphism, and modern weathering (Fig. 2) (Sansom et al., 2010; Bath
127 Enright, 2018; Parry et al., 2018; Purnell et al., 2018). To do so, we will answer the five
128 following questions:

129 • Question 1: What is the stratigraphic distribution of exceptional preservation in the
130 Fezouata Shale?
131 • Question 2: What were the sedimentary surface processes affecting organisms?
132 • Question 3: Under what conditions did decay and diagenetic mineralization take
133 place?
134 • Question 4: What were the post-diagenetic processes?
135 • Question 5: What is the fidelity of preservation in the Fezouata Shale?

136 Answering these questions allows for comparison of the Fezouata Shale communities and
137 their preservation with both the Burgess Shale and the Chengjiang Biota. This comparison is
138 essential to constrain preservation biases within exceptionally preserved biotas and thus to
139 reconstruct early animal ecosystem evolution. This work has implications in understanding
140 the earliest radiations of complex metazoans on Earth from a fresh perspective that accounts
141 for individual preservation biases that were likely operational at each site.

2. Question 1: stratigraphic context – discontinuous occurrences of exceptional preservation

The Fezouata Shale is largely exposed in the Anti-Atlas of Morocco. During the Early Ordovician, this area was located at high latitudes close to the palaeo-South pole (Torsvik and Cocks, 2011, 2013). In the Anti-Atlas, the Ordovician succession (maximum ~2500m thick to the West) was originally divided into four lithostratigraphic groups, which are in stratigraphic order: the Outer Feijas, the First Bani, the Ktaoua, and the Second Bani (Fig. 3) (Choubert, 1942). Following the stratigraphic work of Destombes in the second half of the 20th century, these stratigraphic groups were subdivided into several formations (Fig. 3) (Destombes, 1970, 1971; Destombes et al., 1985). The Fezouata Shale (Tremadocian–Floian) is unconformably deposited over the middle Cambrian Tabanite Group and is conformably overlained by the Zini Formation (late Floian) that is itself overlain by the Tachilla Formation (Darriwilian) (Fig. 3) (Destombes, 1970, 1971; Destombes et al., 1985). The Fezouata Shale is a siltstone-dominated formation outcropping in an area of 900 km^2 in the Zagora region and with a total thickness of ~ 900 m (Martin et al., 2016b, Vaucher et al., 2016) with sandstone layers becoming more common in the upper part of the formation (Vaucher et al., 2016, 2017). Although mineralized fossils were discovered since the early excavations in the first half of the 20th century, exceptional fossil preservation in the Fezouata Shale was not documented until the early years of the 21st century (Van Roy et al., 2010; Lefebvre et al., 2016a). In the Fezouata Shale, the distribution of exceptional preservation is not random. Exceptionally preserved fossils are found in two distinct stratigraphic intervals (Lefebvre et al., 2016a, 2018). Based on acritarchs, conodonts, and graptolites (Gutiérrez-Marco and Martin, 2016; Lehnert et al., 2016; Nowak et al., 2016; Lefebvre et al., 2018), a late Tremadocian age (Tr3) was proposed for the lower, about 70-m thick interval (*A. murrayi* graptolite biozone; Fig. 3).

167 The upper interval is thinner (~50-m thick), and it occurs about 240 m higher in the
168 succession (Lefebvre et al., 2018). Graptolites suggest a mid-Floian age (Fl2) for this upper
169 interval (Fig. 3) (Gutiérrez-Marco and Martin, 2016; Lefebvre et al., 2018). This review
170 focuses on exceptionally preserved material from the lower interval, because it is
171 stratigraphically well constrained (Van Roy et al., 2010; Martin et al., 2016a; Lefebvre et al.,
172 2018). Within this interval, soft-parts are not found everywhere (Saleh et al., 2019). They
173 occur in discontinuous levels with a periodicity of 100,000 years pointing to a possible
174 eccentricity control through seasonality on this type of preservation (Fig. 3) (Saleh et al.,
175 2019). The control of eccentricity on seasonality (Fig. 3) suggests that the conditions favoring
176 this type of preservation were more likely to be ephemeral than permanent (Saleh et al.,
177 2019).
178
179 **3. Question 2: surface processes – *in-situ* burial by distal tempestites**
180 The lithology of the Fezouata Shale varies from claystone to fine-grained sandstone (Vaucher
181 et al., 2016, 2017; Saleh et al., 2020a), while most of the sedimentary succession of this
182 formation is constituted of siltstones (Vaucher et al., 2016, 2017; Saleh et al., 2020a). The
183 sedimentary structures found in the Fezouata Shale are typical of a storm-wave dominated
184 environment (Fig. 4A) (Martin et al., 2016; Vaucher et al., 2016, 2017; Saleh et al., 2020a).
185 These storms were erosive, and their deposits are characterized by the presence of normally
186 graded beds (Fig. 4A, C) (Saleh et al., 2020a), and by oscillatory ripples that were increasing
187 in wavelength from distal (null to millimetric wavelength) to proximal settings (metric to
188 plurimetric wavelength) (Fig. 4B, D) (Vaucher et al., 2016, 2017). Storm-wave deposits are
189 discontinuous in the Fezouata Shale. In proximal settings, a tidal modulation of storm waves
190 occurred and is recorded as a repeated stack of larger (low tide) to smaller (high tide)
191 oscillatory structures within fine-grained sandstones (Fig. 4E) (Vaucher et al., 2017). A

192 statistical correlation between sedimentological data from cores and palaeontological data
193 from outcrops showed that exceptional preservation is associated with one of the most distal
194 facies of the Fezouata Shale (Fig. 5) (Saleh et al., 2020a). This facies is characterized with an
195 abundance of mudstones (i.e. an average of 60% illite
196 $\{(K,H_3O)(Al,Mg,Fe)_2(Si,Al)_4O_{10}[(OH)_2,(H_2O)]\}$, 10% of various chlorite minerals, and 30%
197 siltstones (quartz SiO_2) (Saleh et al., 2019). In this facies, event deposits are not stacked and
198 are separated by background sediments (Saleh et al., 2020a). Furthermore, oscillatory
199 structures are absent indicating that these sediments represent storm-induced deposits in an
200 environment just below the storm wave base (SWB; Fig. 5). Furthermore, exceptionally
201 preserved fossils in this facies are interpreted as autochthonous, because they are occurring
202 right under and not within burial deposits (Fig. 4F, G) (Vaucher et al., 2016; Saleh et al.,
203 2018; 2020a,b). When fossils are disarticulated, this results from in-situ decay rather than
204 transportation, because they do not show any preferential orientation (Fig. 4F) with little
205 evidence of physical abrasion (Martin et al., 2015; Lefebvre et al., 2016a; Saleh et al., 2018;
206 Vannier et al., 2019). In fact, only strong storms are accountable for the accumulation of very
207 coarse siltstones to very fine sandstones in this setting causing an entombment delay and the
208 decay of dead organisms on the seafloor (Saleh et al., 2020a). Due to this pre-burial decay,
209 many fossiliferous intervals yielded hundreds of fossils from which only tens preserved soft-
210 structures (Lefebvre et al., 2019; Saleh et al., 2020a). The rarity of storm-induced deposits in
211 distal settings and its impact on living communities in the Fezouata Shale is validated through
212 observations on body-size fluctuations between sites of this formation (Saleh et al., 2018;
213 2020b). In proximal sites, sessile epibenthic organisms were recurrently buried by storm
214 deposits and could not attain large sizes (Fig. 5). On the contrary nearshore endobenthic taxa
215 were not affected by these events and, if sufficiently motile, they could survive and reach
216 larger sizes (Fig. 5) (Saleh et al., 2018). It was also evidenced that vagile benthic trilobite

taxa, distributed in all fossiliferous environments of the Fezouata Shale, reached larger size in distal settings of this formation due to minimal physical stress in distal environments (Fig. 5) (Saleh et al., 2020b). Some of them possibly migrated during storm seasons from proximal to distal settings (Vannier et al., 2019). However, an increase in body-size for epibenthic taxa from proximal to distal sites of the Fezouata Shale should not be generalized. Specific levels in intermediate settings of this formation are characterized by low diversity assemblages with an abundance of small-sized individuals (Fig. 5) (Martin, 2016; Martin et al., 2016b). This possibly indicates that oxygenation was not stable and periods with lower oxygen concentration existed in these settings, suggesting a temporary or seasonal oxygen minimum zone (OMZ)-like conditions (Fig. 5). This hypothesis needs further testing using a geochemical approach.

4. Question 3: early diagenesis – controlled decay and authigenic mineralization

In the Fezouata Shale there must be some conditions controlling pre-burial decay and compensating for the delay in fossil entombment for exceptional preservation to occur. Pre-burial decay in the Fezouata Shale was controlled and slowed down by a favorable clay mineralogy (Saleh et al., 2019). Chamosite (i.e. originally berthierine) (Fig. 6C) appears to be present in all analyzed levels recording exceptional preservation (i.e. 6 in total), and absent from intervals with skeletal preservation (i.e. 7 levels) (Saleh et al., 2019). Both berthierine and its primary precursor (Anderson et al., 2018) have been shown to slow down decay under experimental conditions with open oxygenic atmospheric diffusion by damaging bacterial cells (McMahon et al., 2016). This may be the main factor that helped some labile anatomies survive delays in entombment by storm-induced deposits in distal facies (Saleh et al., 2019).

When burial occurs, and if it leads to the establishment of anoxic conditions, another type of decay takes place (Fig. 2). Anoxic decay transforms organic matter from decaying carcasses

242 with sulfates SO_4^{2-} from seawater into sulfides H_2S. SO_4^{2-} is not a limiting parameter for this
243 reaction in marine environments. Thus, the H_2S output is mainly controlled by the decay
244 products of biological tissues. High quantities of available organic material such as in the
245 cases of giant decaying arthropods (e.g. 2 meters long *Aegirocassis* radiodonts) leads to the
246 establishment of prominent chemical gradients around carcasses and to the early precipitation
247 and mineral overgrowth around tissues, resulting in their preservation in concretions (Gaines
248 et al., 2012b). However, normal-sized individuals produce less H_2S leading to a less
249 prominent chemical gradient that is not capable of initializing concretion growth (Gaines et
250 al., 2012b). Nevertheless, H_2S can still react with iron from the sediments to form pyrite
251 crystals under anoxic conditions (Raiswell et al., 1993; Schiffbauer et al., 2014). The
252 establishment of anoxic conditions at the time of burial, and H_2S production in the Fezouata
253 Shale lead to the precipitation of framboid and small euhedral crystals in fossils as well as
254 fresh pyrite in non-altered sediments (Fig. 6) (Saleh et al., 2020a). In these sediments, C is
255 also associated with pyrite, possibly suggesting that the original mode of preservation in the
256 Fezouata Shale was comparable to that of the Burgess Shale and the Chengjiang Biota
257 comprising both organic material and authigenic minerals (Gaines et al., 2008; Saleh et al.,
258 2020a,c). As no fossil shows complete pyritization and pyrite precipitation remains rare and
259 tissue-selective, other parameters were also likely controlling pyrite precipitation in the
260 Fezouata Shale (Saleh et al., 2020c). For instance, cuticles of many arthropod taxa are
261 preserved without any pyrite crystals. This can result from H_2S limitation considering that this
262 structure is formed of polysaccharides that are not easily degradable (i.e. quantity of decayed
263 organic matter is not enough to reduce SO_4^{2-}) (Gabbott et al., 2004). However, when
264 comparing internal labile tissues to each other, the model based on H_2S limitation cannot
265 explain why some tissues are pyritized, while others decayed and disappeared (meaning they
266 reduced SO_4^{2-}) without pyritizing (Saleh et al., 2020c). The clue probably lies in Fe

267 availability. Maghemite is found associated with pyrite in some analyzed samples under
268 Raman Spectroscopy (Fig. 6) (Saleh et al., 2020c). Maghemite results from the burial of an
269 original mineral called ferrihydrite $[FeO(OH)]_8[FeO(H_2PO_4)]$ (Mazzetti and Thistlethwaite,
270 2002). Ferrihydrite is a widely distributed biological mineral (Aldred et al., 2009; Hoda et al.,
271 2013; Dunaief et al., 2014). Under anoxic and sulfated conditions, ferrihydrites release high
272 quantities (~ 87%) of reactive Fe (Li et al., 2006) very fast (i.e. half-life of only 2.8 hours)
273 (Canfield et al., 1992). This is 100 times faster than goethite, 270 times faster than hematite
274 and 2000 times faster than reactive silicates (Canfield et al., 1992). For this reason, in order to
275 understand the patterns of exceptional preservation in the Fezouata Shale, but also in
276 Lagerstätten such as Chengjiang and the Beecher's Trilobite Bed in which pyrite played a role
277 in preserving decay-prone anatomies, three parameters should be taken into account: Fe in
278 sediments, Fe in labile tissues, and H_2S production (Saleh et al., 2020c). Accounting for both
279 pre-burial and anoxic decay, different scenarios emerge and are summarized in Fig. 6.

280 • In the first scenario, pre-burial decay is not restricted by any mineralogical phase and
281 burial allowing the establishment of anoxic conditions is delayed. Pyritization does not
282 occur rapidly enough, leaving only body walls (e.g. trilobite carapaces) preserved (Fig.
283 6A).

284 • In the second scenario, burial occurs establishing anoxic conditions for pyritization. Fe in
285 burial material is highly reactive leading to the complete pyritization of the organism, if it
286 is buried alive (Fig. 6B). If the animal decayed on the seafloor but the activity of its
287 degradation was controlled by clay/chlorite minerals, the reactivity of Fe from sediments
288 ensures the pyritization of all tissues that survived pre-burial decay (Fig. 6C). Due to
289 extreme iron reactivity, even carapaces of numerous arthropod taxa that provide small
290 quantities of H_2S are found pyritized in sites such as the Beecher's Trilobite Bed (Briggs
291 et al., 1991; Raiswell et al., 1993, 2008).

- In the third scenario, pre-burial decay is controlled by clay/chlorite minerals. However, after burial, a delay in iron availability in the sediment allows the disappearance of tissues owing to anaerobic decay. The least labile internal tissues will potentially survive anoxic decay and get pyritized once iron from sediments becomes available (Fig. 6D). This scenario explains the selective preservation of guts, while more labile tissues (e.g. nervous systems) are absent (Gutiérrez-Marco et al., 2017).
- In the fourth scenario, pre-burial decay does not occur at all as if animals were buried alive. However, Fe in this scenario is not reactive (even if it is abundant). Thus, only tissues that are rich originally in iron will get preserved and pyritized, even if they are the most labile ones (Fig. 6E). This scenario can explain the preservation of extremely decay-prone structures such as nervous tissues as pyrite replicates in fossils from the Chengjiang Biota (Ma et al., 2012, 2015; Tanaka et al., 2013; Cong et al., 2014).

Considering the decay stages of animals from the Fezouata Shale, the lower availability of iron in sediments in this formation in comparison to sites such as Beecher's Trilobite Bed, and the absence of preserved nervous systems comparable to those occurring in Chengjiang, it is most probable that the taphonomic scenario of most exceptionally preserved fossils found in the Fezouata Shale followed the third scenario (Fig. 6D). However, this pathway is not exclusive, and other scenarios may have accounted for the discovery of only biomineralized parts in some levels from this formation (Fig. 6A). Furthermore, there might have been other parameters facilitating exceptional preservation in the Fezouata Shale. The dominance of storm-induced deposits, the presence of a favorable clay mineralogy and the selective authigenic mineralization surely helped exceptional preservation to occur in this formation. However, these conditions can be acquired in a wide range of marine settings while Ordovician exceptionally preserved biotas remain scarce. The position of the Fezouata Shale

near the South pole in a generally cold water environment might have favored the occurrence of exceptional fossil preservation by slowing down decay rates.

5. Question 4: post-diagenesis – minimal maturation and extensive modern weathering

Raman spectroscopy-based models for thermal maturation on carbon indicate that the Fezouata Shale sediments were buried at maximum temperatures of 200°C (Rahl et al., 2005; Kouketsu et al., 2014; Saleh et al., 2019, 2020a). Thus, metamorphism *sensu stricto* and organic remain volatilization (Fig. 2) did not occur (Saleh et al., 2019, 2020a). In the absence of metamorphism, calcium leaching and the enrichment of manganese in fossils (e.g. Ca leaching from the skeletal elements of solutan echinoderms and the Mn enrichment around the appendages of marrellomorph arthropods (Fig. 7) in the Fezouata Shale are most probably due to modern weathering (Fig. 2). In the Draa Valley, this formation is exposed to abundant water circulation (Warner et al., 2013). Outcrops are surrounded by abandoned terraces and by numerous water wells (Warner et al., 2013). Circulating waters in arid environments with occasional rain falls similar to the Draa Valley are rich in manganese oxides that can start the oxidation of the tissues that were selectively and three dimensionally preserved in pyrite during early diagenesis in addition to the rest of the fossil (Fig. 7A) (Potter and Rossman, 1979; Warner et al., 2013). The resulting products of this reaction are Fe-oxides in the shape of the original pyrite crystals (i.e. euhedral or framboidal) and Mn-sulfates (Fig. 7B) (Larsen and Postma, 1997). If the quantities of Mn are not sufficient to fully oxidize pyrite, pyrite oxidation can further continue through the usage of dissolved oxygen in pore waters (Fig. 7B) and unleash considerable amounts of sulfuric acid (Fig. 7C), thus reducing the pH of the environment and contributing to the dissolution of nearby carbonates (Larsen and Postma, 1997) such as the skeletal elements of echinoderms (Fig. 7D). When extensive weathering occurs by circulating waters that are Fe-rich, C can be completely leached from flattened

fossils and star-shaped iron oxides can be deposited (Fig. 7E) (Saleh et al., 2020a). These star-shaped and modern iron oxides do not result from pyrite oxidation (Fig. 7) (Saleh et al., 2020a) and they account for the red/orange color of many flattened fossils found in the Fezouata Shale (Fig. 1). Although these minerals are weathering products, they lead to an easier differentiation of biological features from the surrounding sediments. This can be evidenced when comparing extensively weathered and less altered fossils belonging to the same animal group such as marrellomorphs (Fig. 7).

6. Question 5: preservation fidelity – underestimation of completely cellular organisms

The Fezouata Shale is major step forward to complete our understanding of the taphonomic mechanisms behind BST preservation in addition to deciphering how these mechanisms influence the patterns of fossil preservation during the Palaeozoic. Burgess Shale-type animals in the Fezouata Biota are preserved just below the SWB. This contrasts with their preservation in much deeper settings during the Cambrian (e.g. the Burgess Shale, Qingjiang Biota) (Gaines, 2014; Fu et al., 2019), and indicates that BST preservation can occur under different bathymetries. Furthermore, the Fezouata Shale shows that BST preservation can occur even if carcasses were exposed on the seafloor prior to their burial as some clay minerals with antibacterial properties can reduce the impact of oxic decay (McMahon et al., 2016; Anderson et al., 2018, 2020a; Saleh et al., 2019). However, this facilitating condition is not enough on its own for soft-structures to preserve because these clay minerals do not stop aerobic bacterial decay; they simply slow it down (McMahon et al., 2016). Most importantly, even if a certain tissue survived oxic degradation it can still decay after burial when different redox conditions and new bacterial communities take over the degradation process (Fig. 6D, E) (Hancy and Antcliffe, 2020). This post-burial degradation can be mitigated by authigenic mineralization such as pyrite or phosphate precipitation (Saleh et al., 2020c; Gueriau et al.,

2020) or even by the association of clay minerals such as kaolinite to certain labile anatomies (Anderson et al. 2020b). Authigenic pyritization happens when iron is available and anoxic conditions are established in sediments, but oxidants from the water column (i.e. sulfates) can still reach decaying carcasses (Raiswell et al., 1993, Saleh et al., 2020c). Carbonate cement, found in many Cambrian Lagerstätten, capping event deposits and blocking oxidants from attaining decaying carcasses, are absent from all sediments in the Fezouata Shale which can explain why pyritization is more abundant in this site than in the Walcott Quarry (Burgess Shale) for example (Saleh et al., 2020a). The last main difference between the Fezouata Shale and most Cambrian Lagerstätten is that fossil transport was not operational at the Ordovician site (Martin et al., 2016a; Vaucher et al., 2016, 2017; Saleh et al., 2018, 2020a, b). All these aforementioned preservational discrepancies indicate that there is no single condition that can be considered as a pre-requisite for BST preservation. BST preservation is a trade-off between decay and mineralization (Fig. 6). This trade-off is controlled by interacting parameters (e.g. transport, oxygen, carbonate cement, specific clay minerals, bacteria). This interaction dictates what and how tissues get preserved in a certain site and the impact of this interaction on preservation can be easily investigated by comparing the co-occurrence of biological structures (Fig. 8A) in these deposits, because all animals are originally made of the same types of structures (e.g. mineralized, cuticularized, cellular, sclerotized) (Saleh et al., 2020d). It has been recently evidenced that biological structure association in the Fezouata Shale is significantly different from that at the Burgess Shale and the Chengjiang Biota (Saleh et al., 2020d). Most taxa in the Walcott Quarry and the Chengjiang Biota preserved two to three types of biological structures at the same time (e.g. cuticle and sclerites; or cuticle, sclerites, and cellular tissues, Fig. 8B) (Saleh et al., 2020d). Most taxa in the Fezouata Shale preserved one type of biological structures at a time (Fig. 8B) (Saleh et al., 2020d). Most importantly, the Fezouata Shale systematically failed to preserve soft cellular structures that are in direct

391 contact with seawater in addition to completely cellular organisms. These results suggest that
392 biodiversity is very likely underestimated in the Fezouata Biota (Fig. 8C) (Saleh et al.,
393 2020d). The absence of these structures can be either linked to (1) the fact that cellular
394 structures in direct contact with sea water (e.g. tentacles of hyoliths) are generally the most
395 labile and the fastest to decay (even when clay minerals with antibacterial properties are
396 present) and/or (2) the lack of required conditions for their mineralization (Saleh et al.,
397 2020d). The magnitude of this underestimation can be quantitively assessed by looking at the
398 proportion of entirely cellular taxa in Cambrian Lagerstätten. In the Walcott Quarry and the
399 Chengjiang Biota, entirely cellular organisms (e.g. chordate, medusoids) constitute 13 and
400 10% respectively of original animal communities in these sites (Saleh et al., 2020d). If the
401 Fezouata Biota had a similar taxonomic composition to the Walcott Quarry and the
402 Chengjiang Biota, the total diversity of this site is most probably underestimated by at least
403 10% (entirely cellular organisms being completely absent). Since this taphonomic bias can be
404 identified and accounted for, the in-situ preservation in the Fezouata Shale becomes an asset
405 for sophisticated ecological studies that examine the evolution of community structure during
406 the Palaeozoic at the transition between the Cambrian Explosion and the Ordovician
407 Radiation. Cambrian ecosystems contrast with Ordovician ones (niche vs dispersal
408 assembled) (Na and Kiessling, 2015; Rasmussen et al., 2019; Stigall et al., 2019). The
409 Fezouata Shale is the only exceptionally preserved biota with hundreds of fossiliferous levels
410 within two stratigraphic intervals (Tremadocian and Floian in age), providing a database that
411 can be used to describe the continuum of ecological change between major Palaeozoic
412 evolutionary events and to decipher if the transition from niche to dispersal-built ecosystems
413 was abrupt or gradual (Harper and Servais, 2018; Rasmussen et al., 2019; Servais et al., 2019;
414 Stigall et al., 2019).
415

7. Conclusions

The Fezouata Shale constitutes a unique record of marine life in the Lower Ordovician. It contains two stratigraphic intervals bearing exceptionally preserved animals (Tremadocian and Floian in age), and documenting an unexpected evolutionary melting pot of Cambrian BST-like holdovers co-occurring with typical members of the Ordovician Radiation. These animals lived in a shallow marine environment that is dominated by storms and were exceptionally preserved *in-situ* just below the SWB. Due to the rarity of storm-induced deposits affecting distal settings, most soft parts decayed prior to their burial. This decay activity was slowed down by a specific clay mineralogy. When favorable conditions for pyritization occurred after burial, pyrite precipitated in specific tissues. In the Fezouata Shale, fossils were originally preserved as carbonaceous compressions with accessory authigenic mineralization in a similar way to Cambrian BST deposits. However, modern water circulation within outcrops leached most of the organic carbon from fossils and oxidized pyrite. Even though the mode of preservation appears to be universal between both Cambrian and Ordovician BST deposits, our review highlights that there are some discrepancies in the mechanisms that lead to this type of preservation. The pre-burial decay in the Fezouata Shale largely contributed to the non-preservation of both soft cellular structures in direct contact with seawater and cellular organisms (e.g. chordates, jellyfish), thus leading to an underestimation of the original diversity of this biota. In spite of this underestimation, the Fezouata Shale is unique in providing an *in-situ*, fully marine community of Burgess Shale-type. The Fezouata Biota represents a series of highly diverse high-latitude communities, at the transition between the Cambrian Explosion and the Ordovician Radiation and as such sits at a critical crossroads in understanding the early evolution of complex animal communities.

Acknowledgments

441 This paper is supported by a grant of the Chinese Postdoctoral Science Foundation awarded to
442 FS. This paper is also a contribution to the TelluS-Syster project 'Vers de nouvelles
443 découvertes de gisements à préservation exceptionnelle dans l'Ordovicien du Maroc' (2017)
444 and the TelluS-INTERRVIE projects 'Mécanismes de préservation exceptionnelle dans la
445 Formation des Fezouata' (2018), and 'Géochimie d'un Lagerstätte de l'Ordovicien inférieur du
446 Maroc' (2019) all funded by the INSU (Institut National des Sciences de l'Univers, France),
447 CNRS. This paper is as well a contribution to the International Geoscience Programme
448 (IGCP) Project 653 – The onset of the Great Ordovician Biodiversification Event. This paper
449 is supported by Grant no. 205321_179084 from the Swiss National Science Foundation,
450 awarded to ACD as Principal Investigator. The authors are particularly grateful to Yves
451 Candela, Lukáš Laibl, Pierre Gueriau, Martina Nohejlovà, Eric Monceret, Stephen Pates,
452 Daniel Vizcaïno, Francesc Pérez-Peris, and Lorenzo Lustri who helped in the field. Orla Bath
453 Enright is thanked for fruitful discussions. Associate Editor Christopher Fielding and two
454 anonymous reviewers are also thanked for their positive comments and insightful reviews.
455

456 **References**

457 Aldred, E.M., Buck, C., Vall, K., Aldred, E.M., Buck, C., Vall, K., 2009. Scientific tests.
458 Pharmacology 331–341. https://doi.org/10.1016/B978-0-443-06898-0.00041-4
459 Anderson, R.P., Tosca, N.J., Gaines, R.R., Mongiardino Koch, N., Briggs, D.E.G., 2018. A
460 mineralogical signature for Burgess Shale–type fossilization. Geology 46, 347–350.
461 https://doi.org/10.1130/G39941.1
462 Anderson, R.P., Tosca, N.J., Cinque, G., Frogley, M.D., Lekkas, I., Akey, A., Hughes, G.M.,
463 Bergmann, K.D., Knoll, A.H. and Briggs, D.E.G, 2020a. Aluminosilicate haloes preserve
464 complex life approximately 800 million years ago. Interface Focus, 10(4), 20200011.
465 Anderson, R.P., Tosca, N.J., Saupe, E.E., Wade, J., Briggs, D.E.G., in press. Early formation

and taphonomic significance of kaolinite associated with Burgess Shale fossils. Geology. doi: https://doi.org/10.1130/G48067.1

Bath Enright, O.G., 2018. Investigating the impacts of transport and decay on the polychaete *Alitta Virens*: Implications for the taphonomy of the Burgess Shale. Unpubl. PhD thesis, University of Portsmouth. p. 305.

Botting, J.P., 2007. 'Cambrian' demosponges in the Ordovician of Morocco: insights into the early evolutionary history of sponges. Geobios 40, 737–748.

Botting, J.P., 2016. Diversity and ecology of sponges in the Early Ordovician Fezouata Biota, Morocco. Palaeogeogr. Palaeoclimatol. Palaeoecol. 460, 75–86.

Briggs, D.E., Bottrell, S.H., and Raiswell, R., 1991. Pyritization of soft-bodied fossils: Beecher's trilobite bed, Upper Ordovician, New York State. Geology 19(12), 1221–1224.

Butterfield, N.J., 1990. Organic preservation of non-mineralizing organisms and the taphonomy of the Burgess Shale. Paleobiology 16(3), 272-286.

Butterfield, N.J., 1995. Secular distribution of Burgess-Shale-type preservation. Lethaia, 28(1), 1-13.

Canfield, D.E., Raiswell, R., Bottrell, S., 1992. The reactivity of sedimentary iron minerals toward sulfide. Am. J. Sci. 292, 659–683. https://doi.org/10.2475/ajs.292.9.659

Choubert, G., 1942. Constitution et puissance de la série primaire de l'Anti-Atlas. C. R. Acad. Sci. Paris 215, 445-447.

Cong, P., Ma, X., Hou, X., Edgecombe, G.D., Strausfeld, N.J., 2014. Brain structure resolves the segmental affinity of anomalocaridid appendages. Nature 513, 538–542. https://doi.org/10.1038/nature13486

Conway Morris, S., 1992. Burgess Shale-type faunas in the context of the 'Cambrian explosion': a review. Journal of the Geological Society 149(4), 631-636.

491 Daley, A.C., Budd, G.E., Caron, J.B., Edgecombe, G.D., Collins, D., 2009. The Burgess
492 Shale anomalocaridid *Hurdia* and its significance for early euarthropod evolution.
493 Science 323, 1597–1600.
494 Daley, A.C., Antcliffe, J.B., Drage, H.B., Pates, S., 2018. Early fossil record of Euarthropoda
495 and the Cambrian Explosion. Proc. Natl. Acad. Sci. 115, 5323–5331.
496 https://doi.org/10.1073/PNAS.1719962115
497 Destombes, J., 1970. Cambrien et Ordovicien. Notes et Mém. Serv. géol. Maroc 229, 161-
498 170.
499 Destombes, J., 1971. L'Ordovicien au Maroc. Essai de synthèse stratigraphique. Mém. Bur.
500 Rech. Géol. Min. 73, 237-263.
501 Destombes, J., Hollard, H., Willefert, S., 1985. Lower Palaeozoic rocks of Morocco, in:
502 Holland, C. (Ed.), Lower Palaeozoic Rocks of the World. John Wiley and Sons,
503 Chichester, pp. 91–336.
504 Duan, Y., Han, J., Fu, D., Zhang, X., Yang, X., Komiya, T., Shu, D., 2014. Reproductive
505 strategy of the bradoriid arthropod *Kunmingella douvillei* from the Lower Cambrian
506 Chengjiang Lagerstätte, South China. Gondwana Res. 25, 983–990.
507 https://doi.org/10.1016/J.GR.2013.03.011
508 Dunaief, D., Cwanger, A., Dunaief, J.L., 2014. Iron-Induced Retinal Damage. Handb. Nutr.
509 Diet Eye 619–626. https://doi.org/10.1016/B978-0-12-401717-7.00063-0
510 Fan, J.X., Shen, S.Z., Erwin, D.H., Sadler, P.M., MacLeod, N., Cheng, Q.M., Hou, X.D.,
511 Yang, J., Wang, X.D., Wang, Y., Zhang, H., Chen, X., Li, G.X., Zhang, Y.C., Shi, Y.K.,
512 Yuan, D.X., Chen, Q., Zhang, L.N., Li, C., Zhao, Y.Y., 2020. A high-resolution
513 summary of Cambrian to early Triassic marine invertebrate biodiversity. Science 367,
514 272–277. https://doi.org/10.1126/science.aax4953
515 Farrell, U.C., Briggs, D.E.G., Gaines, R.R., 2011. Paleoecology of the olenid trilobite

516 *Triarthurus*: new evidence from Beecher's Trilobite Bed and other sites of pyritization.
517 Palaios 26, 730–742. https://doi.org/10.2110/palo.2011.p11-050
518 Fu, D., Tong, G., Dai, T., Liu, W., Yang, Y., Zhang, Y., Cui, L., Li, L., Yun, H., Wu, Y. and
519 Sun, A., 2019. The Qingjiang biota: a Burgess Shale-type fossil Lagerstätte from the
520 early Cambrian of South China. Science 363(6433), pp.1338-1342.
521 Gabbott, S.E., Xian-guang, H., Norry, M.J., Siveter, D.J., 2004. Preservation of Early
522 Cambrian animals of the Chengjiang Biota. Geology 32, 901.
523 https://doi.org/10.1130/G20640.1
524 Gaines, R.R., 2014. Burgess Shale-type preservation and its distribution in space and time.
525 Paleontol. Soc. Pap. 20, 123–146. https://doi.org/10.1017/S1089332600002837
526 Gaines, R.R., Briggs, D.E.G., Yuanlong, Z., 2008. Cambrian Burgess Shale–type deposits
527 share a common mode of fossilization. Geology 36, 755.
528 https://doi.org/10.1130/G24961A.1
529 Gaines, R.R., Hammarlund, E.U., Hou, X., Qi, C., Gabbott, S.E., Zhao, Y., Peng, J., Canfield,
530 D.E., 2012a. Mechanism for Burgess Shale-type preservation. Proc. Natl. Acad. Sci. U.
531 S. A. 109, 5180–4. https://doi.org/10.1073/pnas.1111784109
532 Gaines, R. R., Briggs, D.E.G., Orr, P.J., Van Roy, P., 2012b. Preservation of giant
533 anomalocaridids in silica-chlorite concretions from the Early Ordovician of Morocco.
534 Palaios 27, 317–325. https://doi.org/10.2110/palo.2011.p11-093r
535 Gueriau, P., Bernard, S., Farges, F., Mocuta, C., Dutheil, D.B., Adatte, T., Bomou, B., Godet,
536 M., Thiaudière, D., Charbonnier, S. and Bertrand, L., 2020. Oxidative conditions can
537 lead to exceptional preservation through phosphatization. Geology.
538 Gutiérrez-Marco, J.C., García-Bellido, D.C., 2015. Micrometric detail in palaeoscolecid
539 worms from Late Ordovician sandstones of the Tafilalt Konservat-Lagerstätte, Morocco.
540 Gondwana Res. 28, 875–881. https://doi.org/10.1016/J.GR.2014.04.006

Gutiérrez-Marco, J.C., García-bellido, D.C., Rábano, I., Sá, A.A., 2017. Digestive and appendicular soft-parts, with behavioural implications, in a large Ordovician trilobite from the Fezouata. Sci. Rep. 7, 1–7. https://doi.org/10.1038/srep39728

Gutiérrez-Marco, J.C., Martin, E.L.O., 2016. Biostratigraphy and palaeoecology of Lower Ordovician graptolites from the Fezouata Shale (Moroccan Anti-Atlas). Palaeogeogr. Palaeoclimatol. Palaeoecol. 460, 35–49. https://doi.org/10.1016/J.PALAEO.2016.07.026

Hancy, A.D. and Antcliffe, J.B., 2020. Anoxia can increase the rate of decay for cnidarian tissue: Using *Actinia equina* to understand the early fossil record. Geobiology, 18(2), 167-184.

Harper, D.A. and Servais, T., 2018. Contextualizing the onset of the Great Ordovician Biodiversification Event. Lethaia 51(2), 149-150.

Hoda, K., Bowlus, C.L., Chu, T.W., Gruen, J.R., 2013. Iron metabolism and related disorders. Emery Rimoin's Princ. Pract. Med. Genet. 1–41. https://doi.org/10.1016/B978-0-12-383834-6.00106-3

Hou, X., Siveter, David J., Siveter, Derek J., Aldridge, R.J., Cong, P., Gabbott, S.E., Ma, X., Purnell, M.A., Williams, M., 2004. The Cambrian fossils of Chengjiang, China : the flowering of early animal life. Blackwell.

Kouketsu, Y., Mizukami, T., Mori, H., Endo, S., Aoya, M., Hara, H., Nakamura, D., Wallis, S., 2014. A new approach to develop the Raman carbonaceous material geothermometer for low-grade metamorphism using peak width. Isl. Arc 23, 33–50. https://doi.org/10.1111/iar.12057

Kouraiss, K., El Hariri, K., El Albani, A., Azizi, A., Mazurier, A., Lefebvre, B., 2019. Digitization of fossils from the Fezouata Biota (Lower Ordovician, Morocco): Evaluating computed tomography and photogrammetry in collection enhancement. Geoheritage 11, 1889–1901. https://doi.org/10.1007/s12371-019-00403-z

566 Lamsdell, J.C., Hoşgör, İ., Selden, P.A., 2013. A new Ordovician eurypterid (Arthropoda:
567 Chelicerata) from southeast Turkey: Evidence for a cryptic Ordovician record of
568 Eurypterida. Gondwana Res. 23, 354–366. https://doi.org/10.1016/J.GR.2012.04.006
569 Larsen, F., Postma, D., 1997. Nickel mobilization in a groundwater well field: release by
570 pyrite oxidation and desorption from manganese oxides. Environ. Sci. Technol. 31,
571 2589–2595. https://doi.org/10.1021/ES9610794
572 Lefebvre, B., El Hariri, K., Lerosey-Aubril, R., Servais, T., Van Roy, P., 2016a. The Fezouata
573 Shale (Lower Ordovician, Anti-Atlas, Morocco): a historical review. Palaeogeogr.
574 Palaeoclimatol. Palaeoecol, 460, 7–23.
575 Lefebvre, B., Allaire, N., Guensburg, T.E., Hunter, A.W., Kouraïss, K., Martin, E.L.O.,
576 Nardin, E., Noailles, F., Pittet, B., Sumrall, C.D., Zamora, S., Lefebvre, B., Allaire, N.,
577 Guensburg, T.E., Hunter, A.W., Kouraïss, K., Martin, E.L.O., Nardin, E., Noailles, F.,
578 Pittet, B., Sumrall, C.D., Zamora, S., 2016b. Palaeoecological aspects of the
579 diversification of echinoderms in the Lower Ordovician of central Anti-Atlas, Morocco.
580 Palaeogeogr. Palaeoclimatol. Palaeoecol. 460, 97–121.
581 https://doi.org/10.1016/J.PALAEO.2016.02.039
582 Lefebvre, B., Gutiérrez-Marco, J.C., Lehnert, O., Martin, E.L.O., Nowak, H., Akodad, M., El
583 Hariri, K., Servais, T., 2018. Age calibration of the Lower Ordovician Fezouata
584 *Lagerstätte*, Morocco. Lethaia 51, 296–311. https://doi.org/10.1111/let.12240
585 Lefebvre, B., Guensburg, T.E., Martin, E.L.O., Mooi, R., Nardin, E., Nohejlová, M., Saleh,
586 F., Kouraïss, K., El Hariri, K., David, B., 2019. Exceptionally preserved soft parts in
587 fossils from the Lower Ordovician of Morocco clarify stylophoran affinities within basal
588 deuterostomes. Geobios 52, 27–36. https://doi.org/10.1016/J.GEOBIOS.2018.11.001
589 Lehnert, O., Nowak, H., Sarmiento, G.N., Gutiérrez-Marco, J.C., Akodad, M., Servais, T.,
590 2016. Conodonts from the Lower Ordovician of Morocco—Contributions to age and

591 faunal diversity of the Fezouata *Lagerstätte* and peri-Gondwana biogeography.
592 Palaeogeogr. Palaeoclimatol. Palaeoecol. 460, 50–61.
593 Lei, Q.-P., Han, J., Ou, Q., Wan, X.-Q., 2014. Sedentary habits of Anthozoa-like animals in
594 the Chengjiang *Lagerstätte*: Adaptive strategies for Phanerozoic-style soft substrates.
595 Gondwana Res. 25, 966–974. https://doi.org/10.1016/J.GR.2013.01.007
596 Lerosey-Aubril, R., Paterson, J.R., Gibb, S., Chatterton, B.D.E., 2017. Exceptionally-
597 preserved late Cambrian fossils from the McKay Group (British Columbia, Canada) and
598 the evolution of tagmosis in aglaspidid arthropods. Gondwana Res. 42, 264–279.
599 https://doi.org/10.1016/J.GR.2016.10.013
600 Li, Y.-L., Vali, H., Yang, J., Phelps, T.J., Zhang, C.L., 2006. Reduction of iron oxides
601 enhanced by a sulfate-reducing bacterium and biogenic H2S. Geomicrobiol. J. 23, 103–
602 117. https://doi.org/10.1080/01490450500533965
603 Liu, J., Shu, D., Han, J., Zhang, Z., Zhang, X., 2008. Origin, diversification, and relationships
604 of Cambrian lobopods. Gondwana Res. 14, 277–283.
605 https://doi.org/10.1016/J.GR.2007.10.001
606 Ma, X., Hou, X., Edgecombe, G.D., Strausfeld, N.J., 2012. Complex brain and optic lobes in
607 an early Cambrian arthropod. Nature 490, 258–261. https://doi.org/10.1038/nature11495
608 Ma, X., Cong, P., Hou, X., Edgecombe, G.D., Strausfeld, N.J., 2014. An exceptionally
609 preserved arthropod cardiovascular system from the early Cambrian. Nat. Commun. 5,
610 3560. https://doi.org/10.1038/ncomms4560
611 Ma, X., Edgecombe, G.D., Hou, X., Goral, T., Strausfeld, N.J., 2015. Preservational pathways
612 of corresponding brains of a Cambrian euarthropod. Curr. Biol. 25, 2969–2975.
613 https://doi.org/10.1016/j.cub.2015.09.063
614 Marante, A., 2008. Architecture et dynamique des systèmes sédimentaires silico-clastiques
615 sur la plate-forme géante nord-gondwanienne. Université Michel Montaigne, Bordeaux

616 3. Unpublished.
617 Martin, E., 2016. Communautés animales du début de l'Ordovicien (env. 480 Ma): études
618 qualitatives et quantitatives à partir des sites à préservation exceptionnelle des Fezouata,
619 Maroc. Unpubl. PhD thesis, Université Lyon 1. p.483.
620 Martin, E., Lefebvre, B., Vaucher, R., 2015. Taphonomy of a stylophoran-dominated
621 assemblage in the Lower Ordovician of Zagora area (centrak Anti-Atlas, Morocco). In:
622 Zamora, S., Rabano, I. (Eds.), Progress in Echinoderm Palaeobiology. Cuadernos Mus.
623 Geomin. 19, pp. 95-100.
624 Martin, E.L.O., Pittet, B., Gutiérrez-Marco, J.-C., Vannier, J., El Hariri, K., Lerosey-Aubril,
625 R., Masrour, M., Nowak, H., Servais, T., Vandenbroucke, T.R.A., Van Roy, P., Vaucher,
626 R., Lefebvre, B., 2016a. The Lower Ordovician Fezouata Konservat-Lagerstätte from
627 Morocco: Age, environment and evolutionary perspectives. Gondwana Res. 34, 274–
628 283. https://doi.org/10.1016/J.GR.2015.03.009
629 Martin, E.L.O., Vidal, M., Vizcaïno, D., Vaucher, R., Sansjofre, P., Destombes, J., 2016b.
630 Biostratigraphic and palaeoenvironmental controls on the trilobite associations from the
631 Lower Ordovician Fezouata Shale of the central Anti-Atlas, Morocco. Palaeogeogr.
632 Palaeoclimatol. Palaeoecol. 460, 142–154.
633 https://doi.org/10.1016/J.PALAEO.2016.06.003
634 Mazzetti, L., Thistlethwaite, P.J., 2002. Raman spectra and thermal transformations of
635 ferrihydrite and schwertmannite. J. Raman Spectrosc. 33, 104–111.
636 https://doi.org/10.1002/jrs.830
637 McMahon, S., Anderson, R.P., Saupe, E.E., Briggs, D.E.G., 2016. Experimental evidence that
638 clay inhibits bacterial decomposers: Implications for preservation of organic fossils.
639 Geology 44, 867–870. https://doi.org/10.1130/G38454.1
640 Moysiuk, J., Smith, M.R., Caron, J.-B., 2017. Hyoliths are Palaeozoic lophophorates. Nature

541, 394–397. https://doi.org/10.1038/nature20804

Moysiuk, J., Caron, J.-B., 2019. A new hurdiid radiodont from the Burgess Shale evinces the exploitation of Cambrian infaunal food sources. Proc. R. Soc. B Biol. Sci. 286, 20191079. https://doi.org/10.1098/rspb.2019.1079

Na, L. and Kiessling, W., 2015. Diversity partitioning during the Cambrian radiation. Proceedings of the National Academy of Sciences 112(15), 4702-4706.

Nanglu, K., Caron, J.B., Gaines, R, 2020. The Burgess Shale paleocommunity with new insights from Marble Canyon , British Columbia. Paleobiology 46, 58–81.

Nowak, H., Pittet, B., Vaucher, R., Akodad, M., Gaines, R.R., Vandenbroucke, T.R.A., 2016. Palynomorphs of the Fezouata Shale (Lower Ordovician, Morocco): Age and environmental constraints of the Fezouata Biota. Palaeogeogr. Palaeoclimatol. Palaeoecol. 460, 62–74. https://doi.org/10.1016/J.PALAEO.2016.03.007

Parry, L.A., Smithwick, F., Nordén, K.K., Saitta, E.T., Lozano-Fernandez, J., Tanner, A.R., Caron, J.-B., Edgecombe, G.D., Briggs, D.E.G., Vinther, J., 2018. Soft-bodied fossils are not simply rotten carcasses - Toward a holistic understanding of exceptional fossil preservation. BioEssays 40, 1700167. https://doi.org/10.1002/bies.201700167

Pérez-Peris, F., Laibl, L., Lustri, L., Gueriau, P., Antcliffe, J.B., Bath Enright O.G., Daley, A.C., in press. A new nektaspidid euarthropod from the Lower Ordovician of Morocco. Geological Magazine.

Potter, R.M., Rossman, G.R., 1979. The manganese- and iron-oxide mineralogy of desert varnish. Chem. Geol. 25, 79–94. https://doi.org/10.1016/0009-2541(79)90085-8

Purnell, M.A., Donoghue, P.J.C., Gabbott, S.E., McNamara, M.E., Murdock, D.J.E., Sansom, R.S., 2018. Experimental analysis of soft-tissue fossilization: opening the black box. Palaeontology 61, 317–323. https://doi.org/10.1111/pala.12360

Rahl, J.M., Anderson, K.M., Brandon, M.T., Fassoulas, C., 2005. Raman spectroscopic

carbonaceous material thermometry of low-grade metamorphic rocks: Calibration and application to tectonic exhumation in Crete, Greece. Earth Planet. Sci. Lett. 240, 339–354. https://doi.org/10.1016/J.EPSL.2005.09.055

Raiswell, R., Whaler, K., Dean, S., Coleman, M.., Briggs, D.E.., 1993. A simple three-dimensional model of diffusion-with-precipitation applied to localised pyrite formation in framboids, fossils and detrital iron minerals. Mar. Geol. 113, 89–100. https://doi.org/10.1016/0025-3227(93)90151-K

Raiswell, R., Newton, R., Bottrell, S.H., Coburn, P.M., Briggs, D.E., Bond, D.P., Poulton, S.W., 2008. Turbidite depositional influences on the diagenesis of Beecher's Trilobite Bed and the Hunsrück Slate; sites of soft tissue pyritization. Am. J. Sci. 308, 105–129.

Rasmussen, C.M., Kröger, B., Nielsen, M.L. and Colmenar, J., 2019. Cascading trend of Early Paleozoic marine radiations paused by Late Ordovician extinctions. Proceedings of the National Academy of Sciences 116(15), 7207-7213.

Saleh, F., Candela, Y., Harper, D.A.T., Polechovà, M., Pittet, B., Lefebvre, B., 2018. Storm-induced community dynamics in the Fezouata Biota (Lower Ordovician, Morocco). Palaios 33, 535–541.

Saleh, F., Pittet, B., Perrillat, J., Lefebvre, B., 2019. Orbital control on exceptional fossil preservation. Geology 47, 1–5. https://doi.org/10.1130/G45598.1

Saleh, F., Pittet, B., Sansjofre, P., Guériau, P., Lalonde, S., Perrillat, J.-P., Vidal, M., Lucas, V., EL Hariri, K., Kouraïss, K., Lefebvre, B., 2020a. Taphonomic pathway of exceptionally preserved fossils in the Lower Ordovician of Morocco. Geobios 60. https://doi.org/10.1016/j.geobios.2020.04.001

Saleh, F, Vidal, M., Laibl, L., Sansjofre, P., Gueriau, P., Perez Peris, F., Lustri, L., Lucas, V., Lefebvre, B., Pittet, B., El Hariri, K., Daley, A.C., 2020b. Large trilobites in a stress-free Early Ordovician environment. Geol. Mag. https://doi.org/10.1017/S0016756820000448

691 Saleh, F. Daley, A.C., Lefebvre, B., Pittet, B., Perrillat, J.P., 2020c. Biogenic iron preserves
692 structures during fossilization: A hypothesis. BioEssays 42.
693 https://doi.org/10.1002/bies.201900243
694 Saleh, F., Antcliffe, J.B., Lefebvre, B., Pittet, B., Laibl, L., Perez Peris, F., Lustri, L., Gueriau,
695 P., Daley, A.C., 2020d. Taphonomic bias in exceptionally preserved biotas. Earth Planet.
696 Sci. Lett. 529. https://doi.org/10.1016/j.epsl.2019.115873
697 Sansom, R.S., Gabbott, S.E., Purnell, M.A., 2010. Non-random decay of chordate characters
698 causes bias in fossil interpretation. Nature 463, 797–800.
699 https://doi.org/10.1038/nature08745
700 Schiffbauer, J.D., Xiao, S., Cai, Y., Wallace, A.F., Hua, H., Hunter, J., Xu, H., Peng, Y.,
701 Kaufman, A.J., 2014. A unifying model for Neoproterozoic–Palaeozoic exceptional
702 fossil preservation through pyritization and carbonaceous compression. Nat. Commun. 5,
703 5754. https://doi.org/10.1038/ncomms6754
704 Servais, T., Cascales-Miñana, B., Cleal, C.J., Gerrienne, P., Harper, D.A. and Neumann, M.,
705 2019. Revisiting the Great Ordovician Diversification of land plants: Recent data and
706 perspectives. Palaeogeogr., Palaeoclimatol., Palaeoecol. 534, 109280.
707 Smith, M.R., Caron, J.-B., 2010. Primitive soft-bodied cephalopods from the Cambrian.
708 Nature 465, 469–472.
709 Stigall, A.L., Edwards, C.T., Freeman, R.L. and Rasmussen, C.M., 2019. Coordinated biotic
710 and abiotic change during the Great Ordovician Biodiversification Event: Darriwilian
711 assembly of early Paleozoic building blocks. Palaeogeogr., Palaeoclimatol., Palaeoecol.
712 530, 249-270.
713 Tanaka, G., Hou, X., Ma, X., Edgecombe, G.D., Strausfeld, N.J., 2013. Chelicerate neural
714 ground pattern in a Cambrian great appendage arthropod. Nature 502, 364–367.
715 https://doi.org/10.1038/nature12520

716 Topper, T.P., Greco, F., Hofmann, A., Beeby, A., Harper, D.A.T., 2018. Characterization of
717 kerogenous films and taphonomic modes of the Sirius Passet *Lagerstätte*, Greenland.
718 Geology 46, 359–362. https://doi.org/10.1130/G39930.1
719 Torsvik, T., Cocks, L., 2011. The Palaeozoic palaeogeography of central Gondwana. Geol.
720 Soc. London, Spec. 357, 137–166.
721 Torsvik, T., Cocks, L., 2013. New global palaeogeographical reconstructions for the Early
722 Palaeozoic and their generation. Geol. Soc. London, Mem. 38, 5–24.
723 Van Roy, P., Orr, P.J., Botting, J.P., Muir, L.A., Vinther, J., Lefebvre, B., El Hariri, K.,
724 Briggs, D.E.G., 2010. Ordovician faunas of Burgess Shale type. Nature 465, 215–218.
725 https://doi.org/10.1038/nature09038
726 Van Roy, P., Briggs, D.E. and Gaines, R.R., 2015a. The Fezouata fossils of Morocco; an
727 extraordinary record of marine life in the Early Ordovician. Journal of the Geological
728 Society 172(5), 541-549.
729 Van Roy, P., Daley, A.C., Briggs, D.E.G., 2015b. Anomalocaridid trunk limb homology
730 revealed by a giant filter-feeder with paired flaps. Nature 522, 77–80.
731 https://doi.org/10.1038/nature14256
732 Vannier, J., Vidal, M., Marchant, R., El Hariri, K., Kouraïss, K., Pittet, B., El Albani, A.,
733 Mazurier, A., Martin, E.L.., 2019. Collective behaviour in 480-million-year-old trilobite
734 arthropods from Morocco. Sci. Rep. 9.
735 Vaucher, R., Martin, E.L.O., Hormière, H., Pittet, B., 2016. A genetic link between
736 Konzentrat- and Konservat-*Lagerstätten* in the Fezouata Shale (Lower Ordovician,
737 Morocco). Palaeogeogr. Palaeoclimatol. Palaeoecol. 460, 24–34.
738 https://doi.org/10.1016/J.PALAEO.2016.05.020
739 Vaucher, R., Pittet, B., Hormière, H., Martin, E.L.O., Lefebvre, B., 2017. A wave-dominated,
740 tide-modulated model for the Lower Ordovician of the Anti-Atlas, Morocco.

741 Sedimentology 64, 777–807. https://doi.org/10.1111/sed.12327
742 Vinther, J., Van Roy, P., Briggs, D.E.G., 2008. Machaeridians are Palaeozoic armoured
743 annelids. Nature 451, 185–188. https://doi.org/10.1038/nature06474
744 Vinther, J., Parry, L., Briggs, D.E.G., Van Roy, P., 2017. Ancestral morphology of crown-
745 group molluscs revealed by a new Ordovician stem aculiferan. Nature 542, 471–474.
746 https://doi.org/10.1038/nature21055
747 Warner, N., Lgourna, Z., Bouchaou, L., Boutaleb, S., Tagma, T., Hsaissoune, M., Vengosh,
748 A., 2013. Integration of geochemical and isotopic tracers for elucidating water sources
749 and salinization of shallow aquifers in the sub-Saharan Drâa Basin, Morocco. Appl.
750 Geochemistry 34, 140–151. https://doi.org/10.1016/J.APGEOCHEM.2013.03.005
751 Zhang, X., Liu, W., Zhao, Y., 2008. Cambrian Burgess Shale-type *Lagerstätten* in South
752 China: Distribution and significance. Gondwana Res. 14, 255–262.
753

754 **Figure captions**

755 **Figure 1.** Fossils from the Fezouata Biota. (A) The distribution of classes among fossiliferous
756 levels from the Fezouata Shale. (B) Xiphosuran chelicerate indet. AA.TER.OI.3, (C) hyolith
757 with preserved internal parts YPM515750, (D) *Bavarilla* sp., trilobite with preserved antennae
758 AA.BIZ15.OI.16, (E) *Furca*, marrellomorph arthropod AA.BIZ31.OI.39, (F) *Palaeoscolex*?
759 *tenensis*, palaeoscolecid worm, AA.BGF2.OI.1, (G) Aglaspidid arthropod, AA-TER-OI-5,
760 (H) *Pirania auraeum*, demosponge AA.JBZ.OI.115, (I) *Thelxiope*-like arthropod YPM
761 226544, (J) *Taricciocia tazagurtensis*, liwiid arthropod, MGL102155a, (K) *Bohemiaecystis* sp.,
762 stylophoran echinoderm with preserved soft tissues including the water vascular system
763 AA.BIZ15.OI.259, (L) frontal appendages of *Aegirocassis benmoulae*, radiodont arthropod
764 YPM 527123. AA: University Cadi-Ayyad, Marrakesh, YPM: Yale Peabody Museum, MGL:
765 Lausanne University.

766 **Figure 2.** Processes and pathways involved during the transfer of organic matter from the
767 biosphere into the lithosphere (i.e. fossilization). These processes determine which characters
768 from the original morphology are lost or retained (Sansom et al., 2010; Bath Enright, 2018;
769 Parry et al., 2018; Purnell et al., 2018).
770 **Figure 3.** Ordovician lithostratigraphic sequencing of the Zagora area (modified from
771 Marante, 2008) completed with graptolite biostratigraphy for the Fezouata Shale (based on
772 Gutiérrez-Marco and Martin, 2016). Exceptionally preserved fossils occur discontinuously
773 (every 100,000 years) within eccentricity-controlled levels belonging to two stratigraphic
774 intervals (Saleh et al., 2019).
775 **Figure 4.** Sedimentary structures in the Fezouata Shale, typical of a storm-wave dominated
776 environment. (A) Storm bed surrounded by background sediments, (B) bed surface displaying
777 2D oscillatory ripples of centimetric wavelength, (C) storm beds displaying a normal grading,
778 (D) hummocky cross-stratified sandstone showing a metric wavelength, (E) In shallower
779 settings, a tidal modulation of storm waves occurs and is recorded as a repeated stack of
780 larger (low tide) to smaller (high tide) oscillatory structures within fine-grained sandstone, (F)
781 In distal settings, fossils were decaying on the seafloor prior to their burial by storm-induced
782 deposits. Disarticulated skeletal elements of the rhombiferan echinoderm *Macrocystella*
783 *bohemica* in green, trilobites in blue, bioturbations in pink, and undetermined elements in
784 beige, (G) most exceptionally preserved BST fossils are preserved *in-situ* under storm-
785 induced beds. Some shelly organisms can be preserved within background sediments because
786 they are resistant to decay and they do not require an event deposition (Kouraiss et al., 2019;
787 Vannier et al., 2019; Saleh et al., 2020a).
788 **Figure 5.** Body size variations of epibenthic, shallow endobenthic, and deep endobenthic taxa
789 along the proximal-distal axis of the Fezouata Shale accordingly with differences in burial
790 rates and oxygenation (OMZ= Oxygen Minimum Zone; SWB: Storm Wave Base).

Figure 6. Different scenarios of decay and mineralization according to a model based on Fe availability in biological tissues, Fe reactivity in the sediments and H_2S production (Saleh et al., 2020c). (A) Absence of pyrite precipitation due to a delay in burial (*Platypeltoides magrebiensis* trilobite; AA.TGR0a.OI.132). (B, C) Most of the organism is pyritized including the body wall (*Triarthrus eatoni* trilobite; YPM.516160) (Farrell et al., 2011). (D) Pyritized parts of the digestive system (*Megistaspis hammondi* trilobite*;* MGM.6755X) (Gutiérrez-Marco et al., 2017). (E) Pyritized nervous system preserved as a dark brown/black imprint (*Fuxanhuia protensa* arthropod; YKLP.15006) (Ma et al., 2015). The purple spectrum is indicative of chamosite/berthierine identified using X-Ray Diffraction. The red arrows and boxes are examples of pyritized areas identified using Raman Spectroscopy and Backscattered Electronic Microscopy on fossils and fresh sediments. Orange boxes are examples of carbonaceous preservation identified under Raman Spectroscopy and Backscattered Electronic Microscopy as well. MGM: Museo Geominero, Madrid, YKLP: Yunnan Key Laboratory for Paleobiology.

Figure 7. Modern weathering effect on fossils from the Fezouata Shale. Manganese oxides start the oxidation process (A) followed by dissolved oxygen in pore waters (B). The resulting products of these reactions are respectively manganese sulfates (B) and sulfuric acid (C). Sulfuric acid leaches calcium from the skeletal elements of the fossils (D). If extensive weathering occurs, all C is leached from fossils and replaced by modern, star shaped iron oxides from circulating water (E). This process explains the absence of Ca in the skeleton of a solutan echinoderm (CASG72938) and the enrichment in Mn- deposits surrounding the extensively weathered marrellomorph (AA.BIZ31.OI.39). Modern star-shaped iron oxides that are deposited during this process gave the extensively weathered marrellomorph a red/orange color in comparison to the less weathered marrellomorph (AA.BIZ15.OI.364). CASG: California Academy of Sciences.

Figure 8. (A) *Branchiocaris pretiosa*, a crustacean arthropod from the Burgess Shale USNM189028nc preserving three types of biological structures. (B) Differences in the preservational pattern between the Fezouata Shale and the Burgess Shale and the Chengjiang Biota (Saleh et al., 2020d). (C) Exceptionally preserved biotas during the Cambrian and Ordovician plotted on the global diversity curve from Rasmussen et al. (2019). Note that the Fezouata Shale does not preserve completely cellular organisms such as cambroernids and chordates; Cambrian Explosion (CE), Ordovician Radiation (OR). USNM: United States National Museum of Natural history.

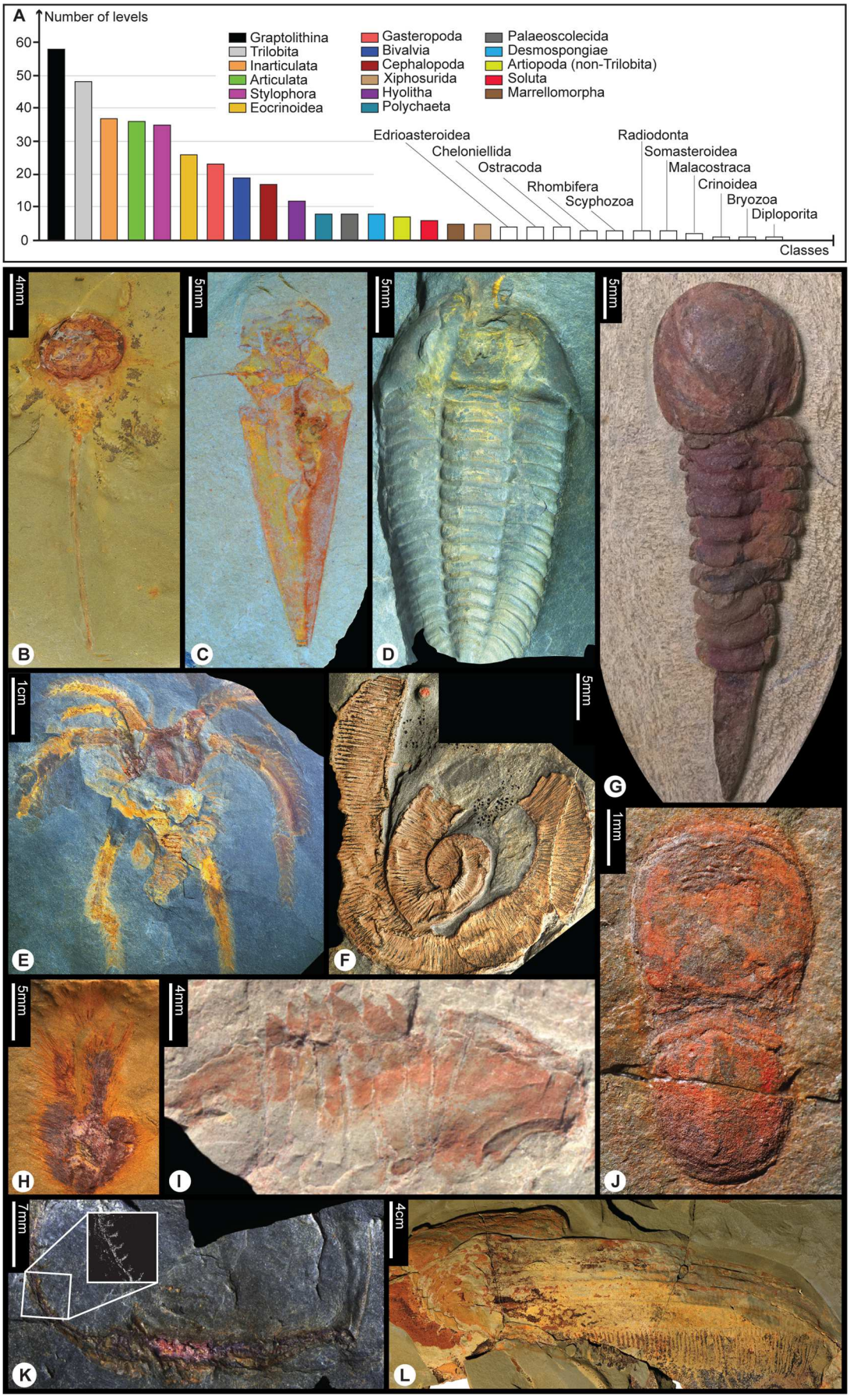

824

825 **Figure 1**

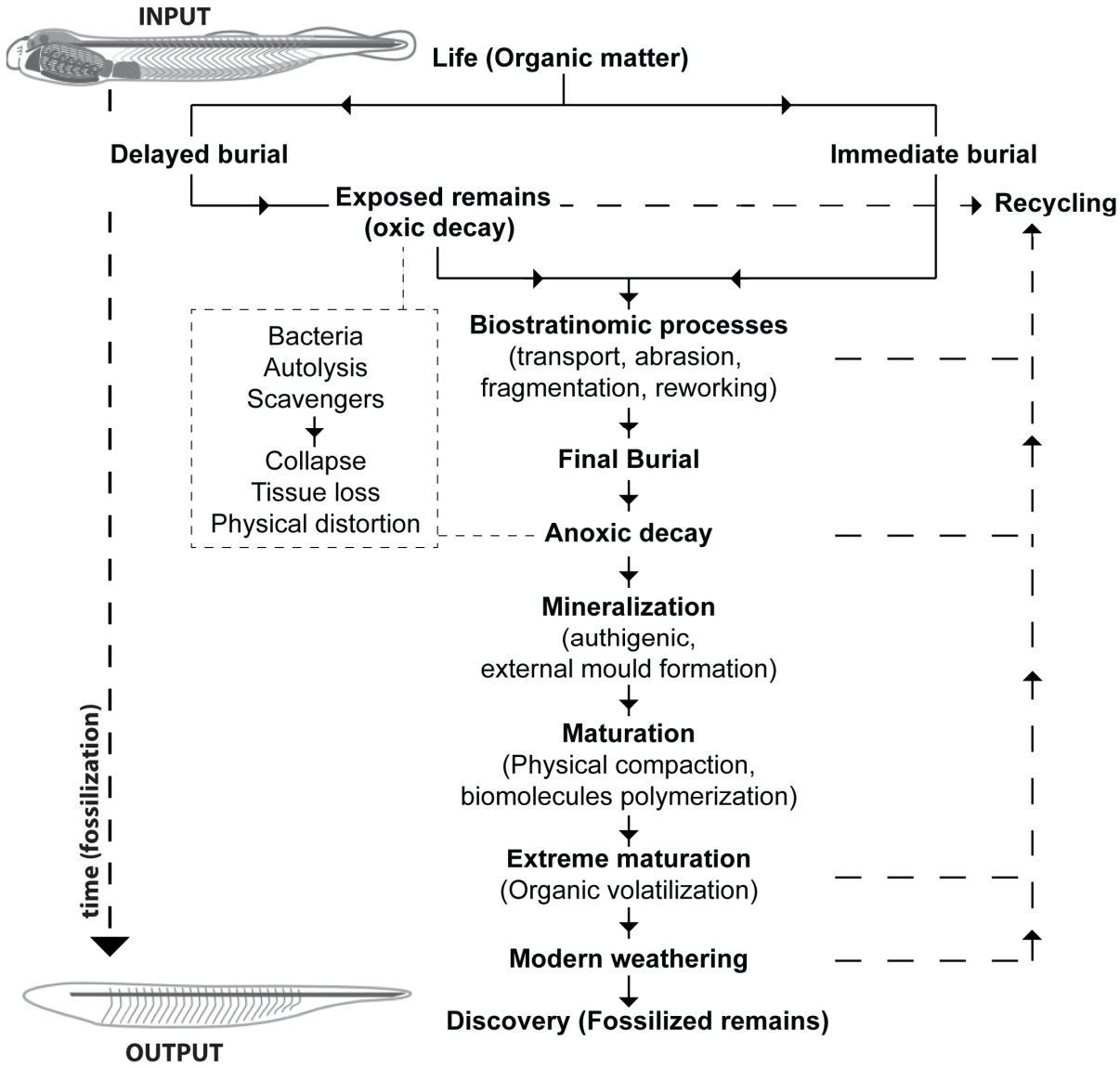

826

827 **Figure 2**

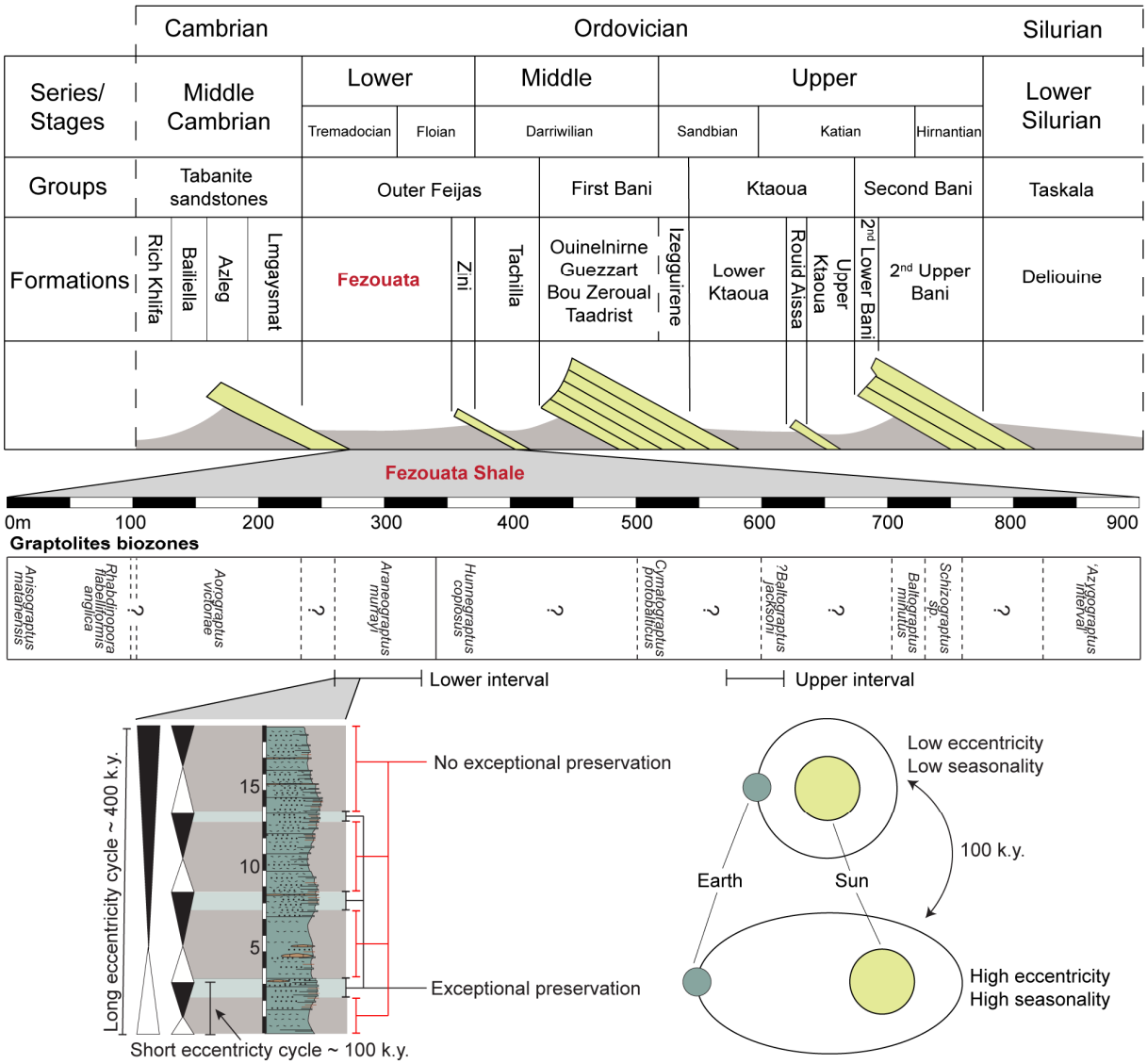

828

829 **Figure 3**

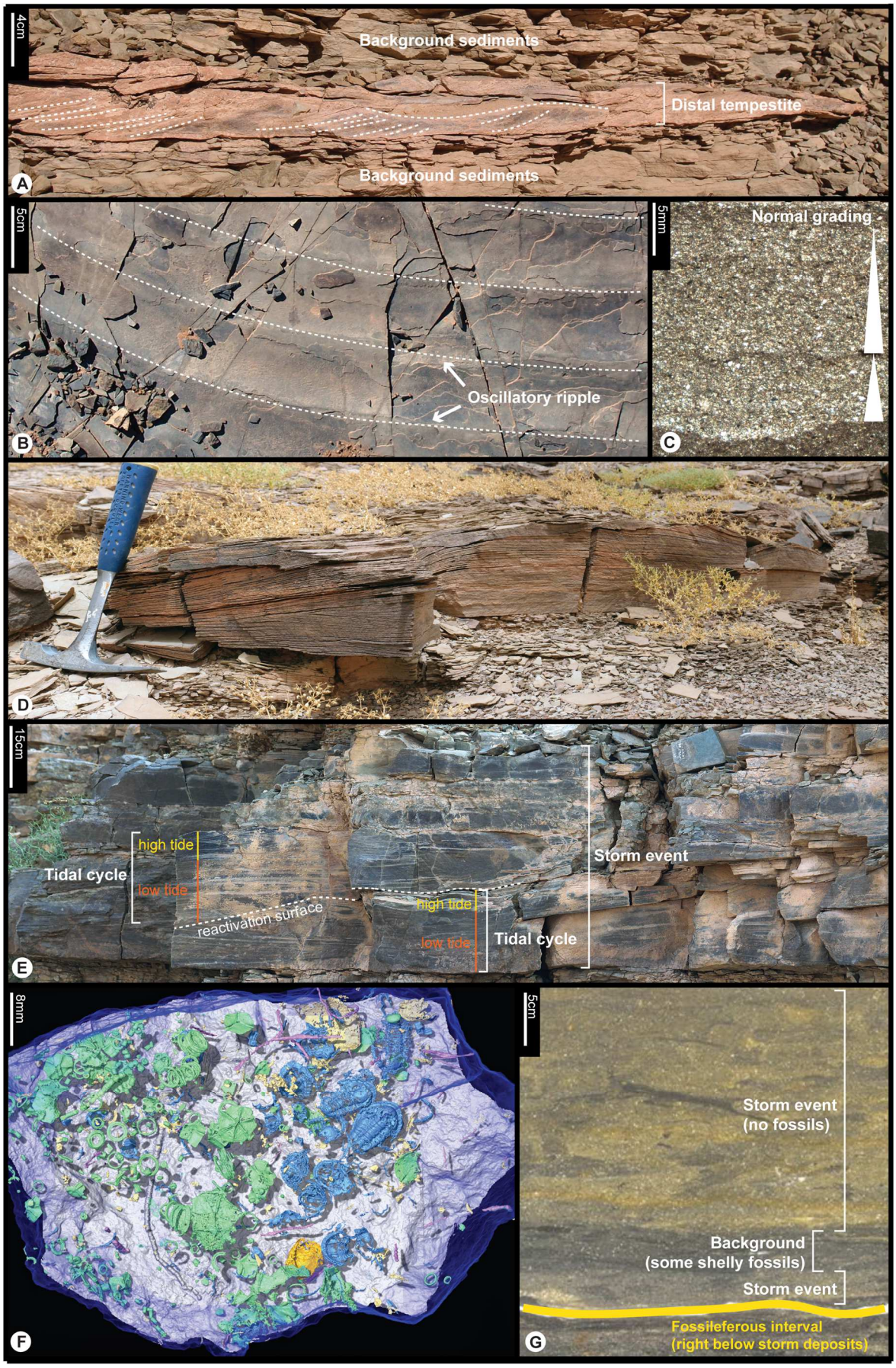
4cm
Background sediments
Distal tempestite
Background sediments
A
5cm
Oscillatory ripple
B
5mm
Normal grading
C
D
15cm
high tide
Tidal cycle
low tide
reactivation surface
high tide
low tide
Tidal cycle
Storm event
E
8mm
F
5cm
Storm event
(no fossils)
Background
(some shelly fossils)
Storm event
Fossiferous interval
(right below storm deposits)
G

Figure 4

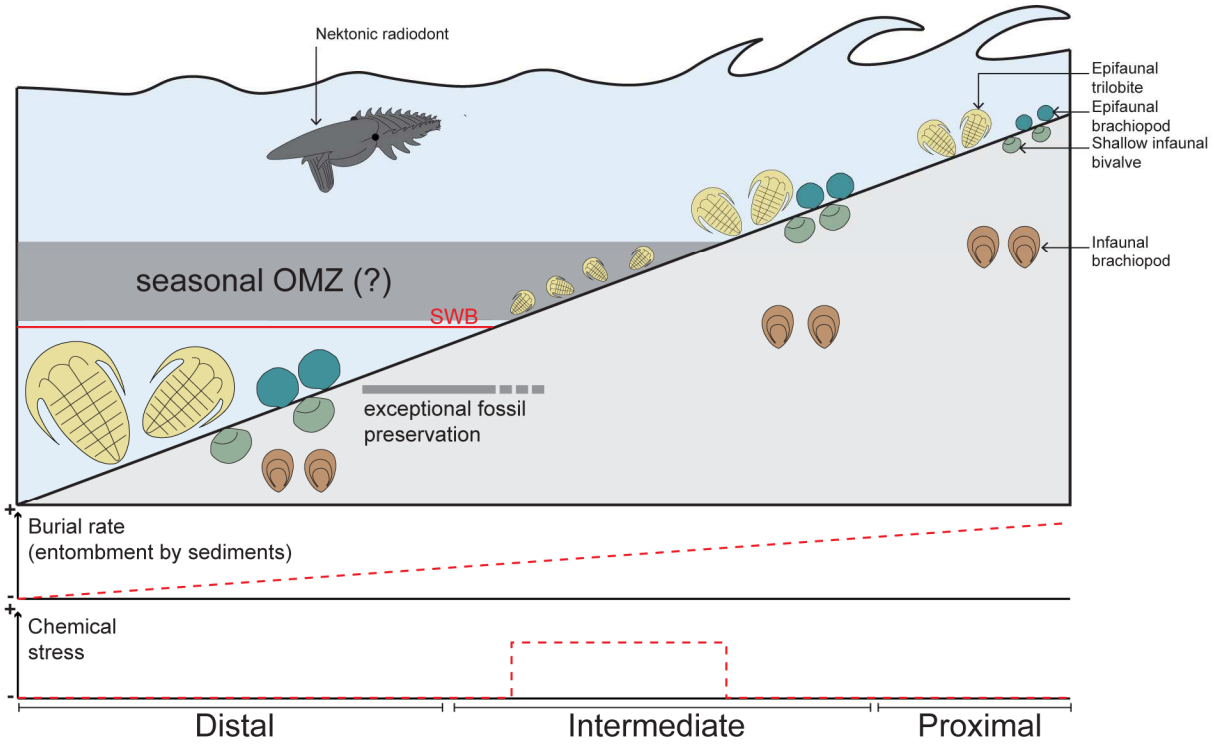

832

833 **Figure 5**

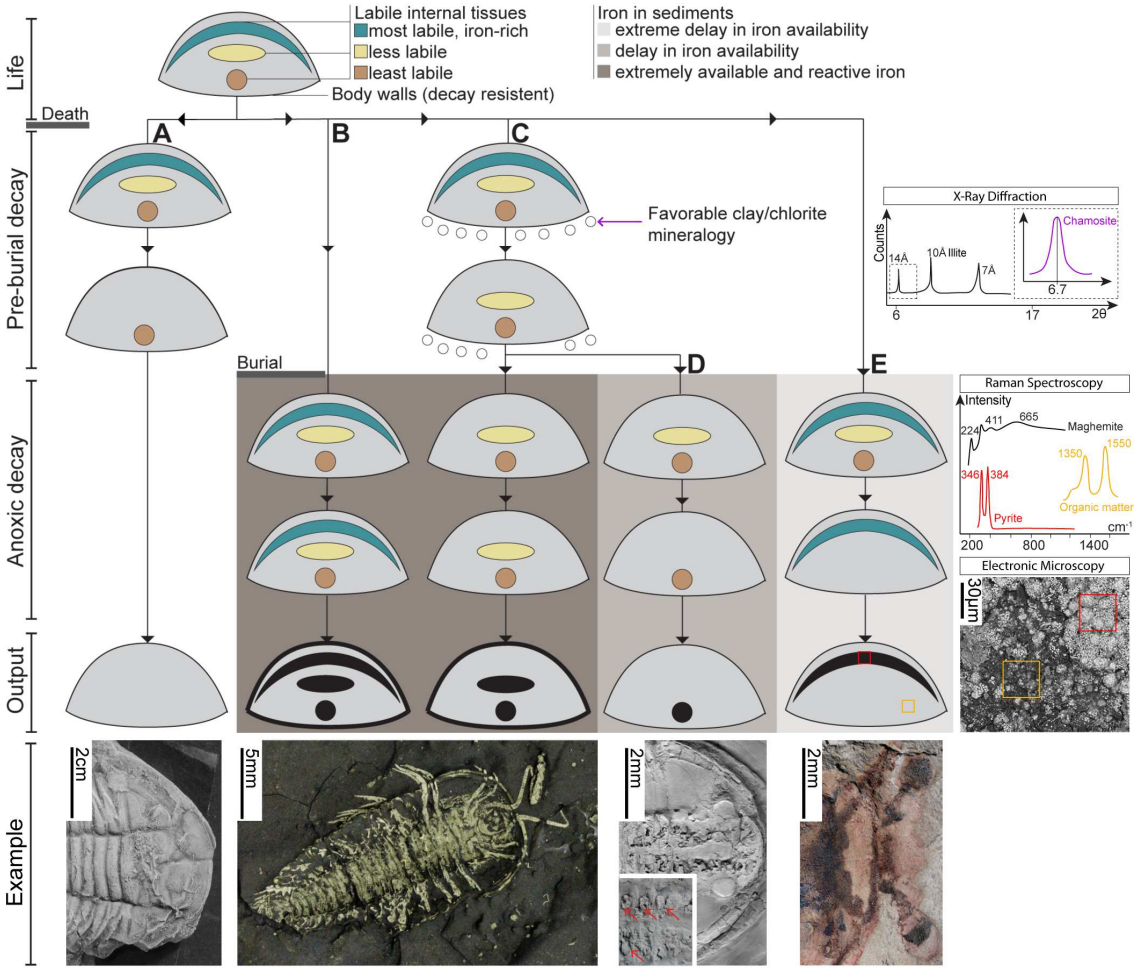

834

835 **Figure 6**

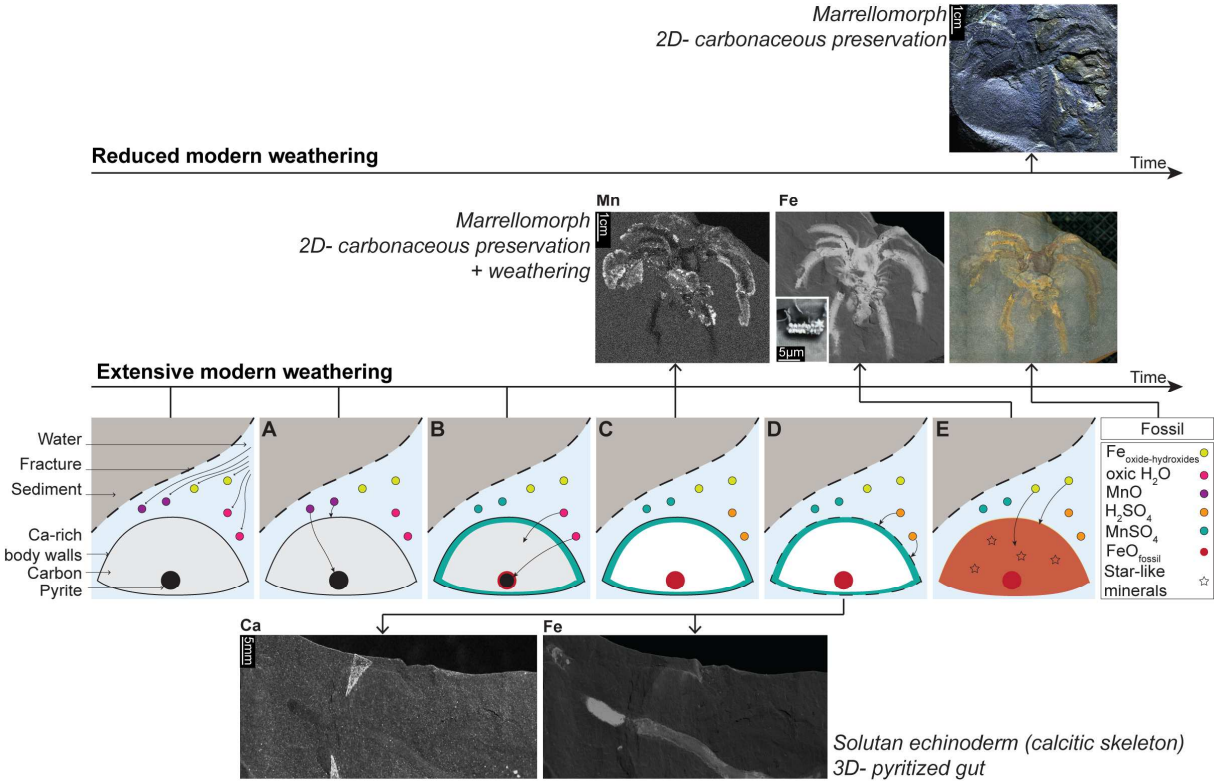

836

837 **Figure 7**

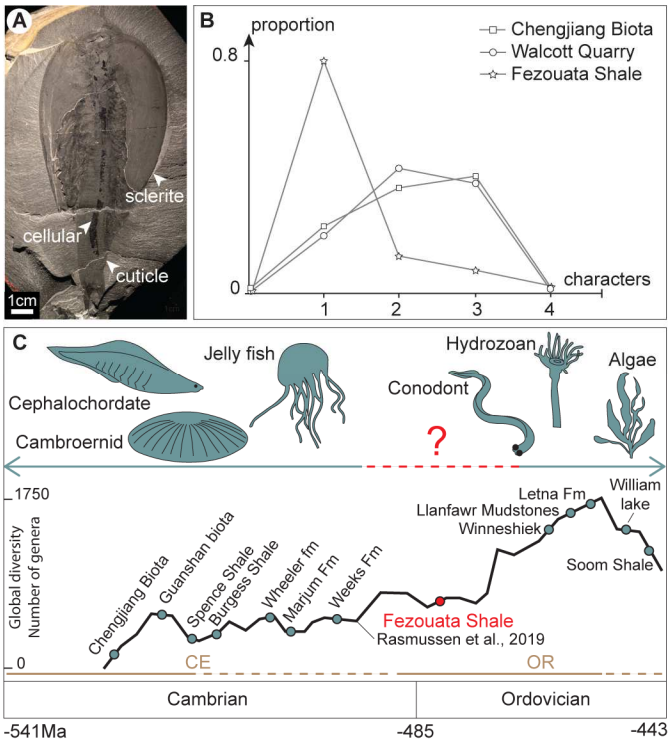

838

839 **Figure 8**